Biochemical and Biophysical Research Communications 460 (2015) 957–963

Contents lists available at ScienceDirect

Biochemical and Biophysical Research Communications

journal homepage: www.elsevier.com/locate/ybbrc

Crystal structure of human POP1 and its distinct structural feature for PYD domain

Jae Young Choi [a, 1], Chang Min Kim [a, 1], Eun Kyung Seo [a, 1], Eijaz Ahmed Bhat [a], Tae-ho Jang [a], Jun Hyuck Lee [b, c], Hyun Ho Park [a, *]

[a] School of Biotechnology and Graduate School of Biochemistry at Yeungnam University, Gyeongsan 712-749, South Korea
[b] Division of Polar Life Sciences, Korea Polar Research Institute, Incheon 406-840, Republic of Korea
[c] Department of Polar Sciences, Korea University of Science and Technology, Incheon 406-840, Republic of Korea

ARTICLE INFO

Article history:
Received 11 March 2015
Available online 1 April 2015

Keywords:
Innate immunity
Inflammation
Inflammasome
POP1
Crystal structure
PYD domain

ABSTRACT

Inflammatory caspases, such as caspase-1, which is critical for the innate immune response, are activated upon the formation of a molecular complex called the inflammasome. The inflammasome is composed of three proteins, the Nod-like receptor (NLRP, NLRC or AIM2), apoptosis associated speck-loke protein containing a caspase-recruitment domain (ASC), and caspase-1. ASC is an adaptor molecule that contains an N-terminal PYD domain and a C-terminal CARD domain for interaction with other proteins. Upon activation, the N-terminal PYD of ASC homotypically interacts with the PYD domain of the Nod-like receptor, while its C-terminal CARD homotypically interacts with the CARD domain of caspase-1. PYD only protein 1 (POP1) negatively regulates inflammatory response by blocking the formation of the inflammasome. POP1 directly binds to ASC via a PYD:PYD interaction, thereby preventing ASC recruitment to Nod-like receptor NLRPs. POP1-mediated regulation of inflammation is of great biological importance. Here, we report the crystal structure of human POP1 and speculate about the inhibitory mechanism of POP1-mediated inflammasome formation based on the current structure.

1. Introduction

For proper immune responses, the activation of inflammatory cytokines, such as IL-1b and IL-17, which are produced as procytokines and have to be processed by enzymes to be activated, is critical [1–3]. The processed, matured, and fully functional inflammatory cytokines can be produced by inflammatory caspases, such as caspase-1 and caspase-5, which are activated by the formation of large molecular complexes known as inflammasomes [4,5]. Inflammasomes are composed of three proteins, a NOD-like receptor (NLR), ASC (apoptosis-associated speck-like protein containing a caspase-recruitment domain) and caspase-1 [5,6]. Pathogen-associated molecular patterns (PAMPs) or damage-associated molecular patterns (DAMPs) can trigger the formation of inflammasomes during innate immune response [7,8]. The death domain (DD) superfamily, which is one of the largest classes of protein-interaction domains and is particularly involved in the protein interactions of apoptosis and the inflammation signaling pathway, plays a critical role in the assembly of the inflammasome [9]. The DD superfamily comprises the death domain (DD) subfamily, the death effector domain (DED) subfamily, the caspase recruitment domain (CARD) subfamily and the pyrin domain (PYD) subfamily [10–12]. PYD-containing NLRs, such as NLRP3, sense multiple danger signals, including bacteria and microbial toxins, directly or indirectly. The adaptor molecule ASC contains two protein-interaction modules, PYD at the N-terminus and CARD at the C-terminus. Caspase-1 has a CARD domain at the N-terminus. During inflammasome formation, ASC interacts directly with NALP3 via a PYD:PYD interaction and with caspase-1 via a CARD:CARD interaction [5,13]. Inflammasomes are targets for the development of new anti-inflammatory drugs for the treatment of chronic inflammatory disease [13,14].

PYD-only proteins, including POP1, POP2, and POP3, have been identified as regulators of inflammation and innate immunity due to their effect on the assembly of the inflammasome [15,16]. POP1, which shows 64% sequence identity to the PYD of ASC, directly interacts with ASC to inhibit the interaction between ASC and NLRPs, while POP2 binds to NLRPs to prevent inflammasome formation (Fig. 1A). Several viruses, including the pox virus, the

* Corresponding author. School of Biotechnology, Graduate School of Biochemistry, Yeungnam University, South Korea. Fax: +82 053 810 4769.
E-mail address: hyunho@ynu.ac.kr (H.H. Park).
[1] These authors contributed equally to this work.

http://dx.doi.org/10.1016/j.bbrc.2015.03.134
0006-291X/

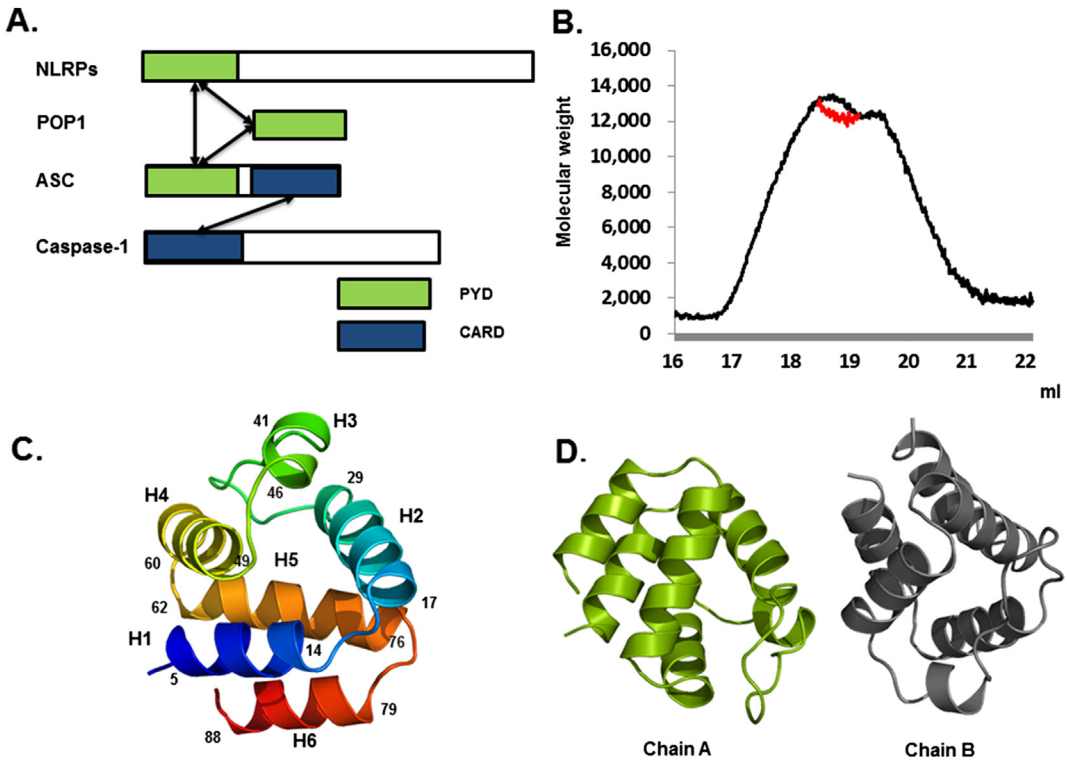

Fig. 1. Crystal structure of POP1. A. Domain boundary of inflammasome components. Domains involved in protein interactions are shown. Black arrows indicate specific interactions. B. Determination of the molecular mass of the POP1 by multi-angle light scattering (MALS). C. Ribbon diagram of POP1. The chain is colored by the spectrum from blue to red from the N– to C–termini. Helices H1 to H6 are labeled. Numbers indicate the amino acid residues that start and end of each helix. D. Dimer structure of POP1. Chain A (light green color) and Chain B (gray color) are shown separately. (For interpretation of the references to colour in this figure legend, the reader is referred to the web version of this article.)

myxoma virus, and the Shope fibroma virus, contain viral POPs to suppress the host immune response [17,18]. Viral POPs can target inflammasomes. Given that POP-mediated regulation of inflammation and innate immunity are interesting features of the regulation of the immune response and are associated with many human diseases, including immune disorders, studies of these protein interactions are of great biological importance. In this study, we report the crystal structure of POP1 at 2.7 Å resolution. Although POP1 has a canonical six-helix bundle structural fold similar to other PYD domains, our crystal structure also shows novel features. By structural comparison, we found that the structure of the POP1 PYD is more closely related to the structure of DEDs rather than DD or CARD domains within the DD superfamily. We also identified the distinct structural features of the PYD

Table 1
Crystallographic statistics.

Data collection	Se-Met	Native
Space group	$P2_13$	$P2_13$
Cell dimensions		
a, *b*, *c*	94.1 Å, 94.1 Å, 94.1 Å	94.4 Å, 94.4 Å, 94.4 Å
Resolution	50–3.6 Å	50-2.7 Å
[a]R_{sym}	18.7% (55.0%)	10.1% (42.6%)
[a]$I/\sigma I$	39.6 (5.4)	38.6 (4.1)
[a]Completeness	100% (100%)	99.9% (100%)
[a]Redundancy	6.3 (6.2)	6.8 (6.5)
Refinement		
Resolution	38-2.7 Å	
No. reflections used (completeness)	4116 (99.7%)	
R_{work}/R_{free}	23.3%/30.3%	
No. atoms		
Protein	1390	
Water	22	
Average B-factors		
Protein	20.8 $Å^2$	
Water and other small molecules	9.8 $Å^2$	
R.M.S. deviations		
Bond lengths	0.010 Å	
Bond angles	1.375°	
Ramachandran plot		
Most favored regions	95.88%	
Additional allowed regions	4.12%	

[a] Highest resolution shell is shown in parentheses.

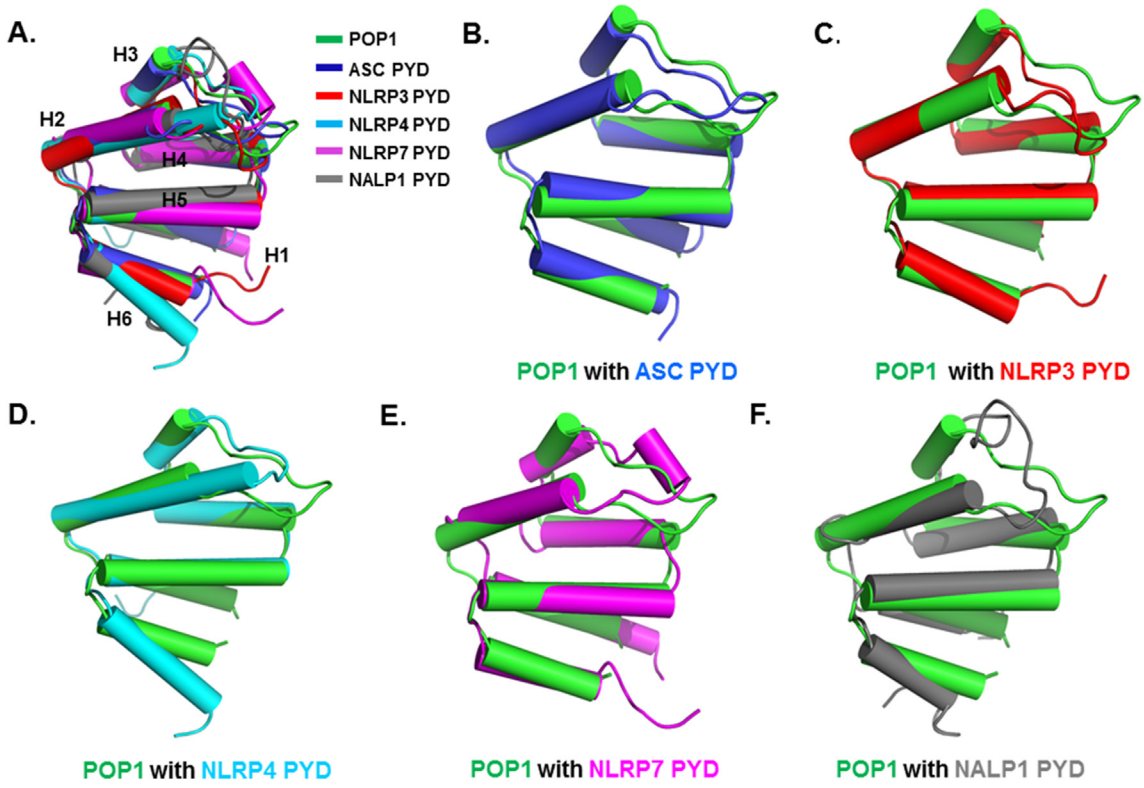

Fig. 2. Superposition of POP1 with other PYDs. A. POP1 (green) and five structurally homologous PYDs are superimposed. B–F. Pairwise structural comparisons were also performed. POP1 is green, and ASC PYD is blue (B), NLRP3 PYD is red (C), NLRP4 PYD is cyan (D), NLRP7 PYD is magenta (E), and NALP1 PYD is gray (F). (For interpretation of the references to colour in this figure legend, the reader is referred to the web version of this article.)

compared with the DED. Finally, based on the structure of POP1 and the recently described EM structures of the ASC filament and the ASC PYD:NLRP3 PYD complex [19], we speculate on the mechanism by which POP1 inhibits the formation of the inflammasome.

2. Materials and methods

2.1. Protein expression and purification

The details of the expression and purification methods for POP1 used in this study have been introduced at previous study [20]. Briefly, human POP1 (amino acids 1–89) was amplified by PCR and inserted into the homemade pOKD vector [25]. The plasmid was then expressed in BL21 (DE3) *E. coli* competent cells by overnight induction with 0.5 mM isopropyl-D-thiogalactopyranoside (IPTG). The target protein, which contained a C-terminal His-tag, was purified by two-step chromatography, nickel-affinity and gel-filtration chromatography, using a Superdex200 gel filtration column (GE Healthcare, Waukesha, WI, USA) that had been pre-equilibrated with a solution of 20 mM Tris at pH 8.0 and 500 mM NaCl. The eluted target protein was pooled and concentrated to 7–8 mg ml^{-1}.

2.2. Crystallization and data collection

The crystallization conditions were initially screened by the hanging drop vapor-diffusion method using various screening kits. The best crystals were grown by equilibrating a mixture containing 1 μl of protein solution (7–8 mg ml^{-1} protein in 20 mM Tris at pH 8.0, 500 mM NaCl) and 1 μl of a reservoir solution containing 3.6 M sodium formate and 0.1 M Tris–HCl at pH 8.5 against 0.4 ml of reservoir solution. Selenomethionine-substituted POP1 was produced using a previously established method [21] and crystallized similarly. A single-wavelength anomalous diffraction (SAD) data set was collected at the 5C beamline at Pohang Accelerator Laboratory (PAL), Republic of Korea. Data processing and scaling were carried out using the HKL2000 package [22].

2.3. Structure determination and analysis

Selenium positions were found with HKL2MAP [23] using the dataset collected at the peak wavelength. SOLVE and RESOLVE programs were used for Phase calculation and phase improvement [24]. Approximately 70% of the structure was auto-traced. COOT

Table 2
Structural similarity search using DALI [39].

Proteins and accession numbers	Z-score	RMSD (Å)	Identity (%)	References
ASC PYD (1UCP)	15.6	1.2	63	[36]
NLRP3 PYD (3QF2)	14.8	1.8	28	[6]
NLRP4 PYD (4EWI)	12.9	1.9	23	[37]
NLRP7 PYD (2KM6)	12.5	1.8	24	[38]
NLRP12 PYD (2L6A)	10.6	2.2	28	[39]
vFLIP DED (2BBR)	9.3	2.0	20	[40]
NALP1 PYD (1PN5)	9.2	2.3	26	[41]
FADD DED (1A1W)	9.0	2.1	18	[42]

was used for model building and refinement [25] and PHENIX [26], respectively. Final geometry was checked by PROCHECK. Refinement statistics are summarized in Table 1. Ribbon diagrams and molecular surface representations were generated using the Pymol Molecular Graphics System (2002; DeLano Scientific, San Carlos, USA).

2.4. Sequence alignment

The amino acid sequence of PYDs was analyzed using Clustal W (http://www.ebi.ac.kr/Tools/clustalw2/index.html).

2.5. MALS

The absolute molar mass of POP1 was determined using MALS. Highly purified POP1 was injected onto a Superdex200 HR 10/30 gel filtration column (GE Healthcare) that had been equilibrated with buffer containing 20 mM Tris HCl and 500 mM NaCl. The chromatography system was coupled to a MALS detector (miniDAWN EOS) and a refractive index detector (Optilab DSP) (Wyatt Technology, Santa Barbara, CA, USA).

2.6. Protein data bank accession code

Coordinates and structure factors have been deposited in the Protein Data Bank (www.rcsb.org) under accession code 4QOB.

3. Results and Discussion

3.1. Crystal structure of POP1

The absolute molecular weight of highly purified human POP1 was determined by multi-angle light scattering (MALS). The theoretical monomeric molecular weight of POP1, including the C-terminal His-tag, was 11,303 Da, while the experimental molecular weight of MALS was 12,840 KDa (2.5% fitting error), indicating that POP1 exists as monomer in solution (Fig. 1B). Although several PYD structures that could be used as a model structure for molecular replacement (MR) are available, MR was not able to successfully solve the structure of POP1. Instead of using MR, we determined the 2.7 Å crystal structure of POP1 using single-wavelength anomalous diffraction (SAD) and refined the model to an R_{work} of 23.3% and R_{free} of 30.3%. The high-resolution structure of POP1 showed that it forms the canonical six-helical bundle fold (from H1 to H6) is characteristic of the DD superfamily (Fig. 1C). There was one dimer in the asymmetric unit, with the chains classified as chain A and chain B (Fig. 1D). Model chains were built from residue 3 to residue 89. Chain A and Chain B formed an asymmetric dimer. There were no apparent interactions between two chains. H3 and H6 were shorter than other helices. The N and C termini of POP1 were located on the same side of the molecule. The six helices comprising residues 5–14, 17–29, 41–46, 49–60, 62–76, and 79–88 were numbered H1, H2, H3, H4, H5, and H6 (Fig. 1C). One

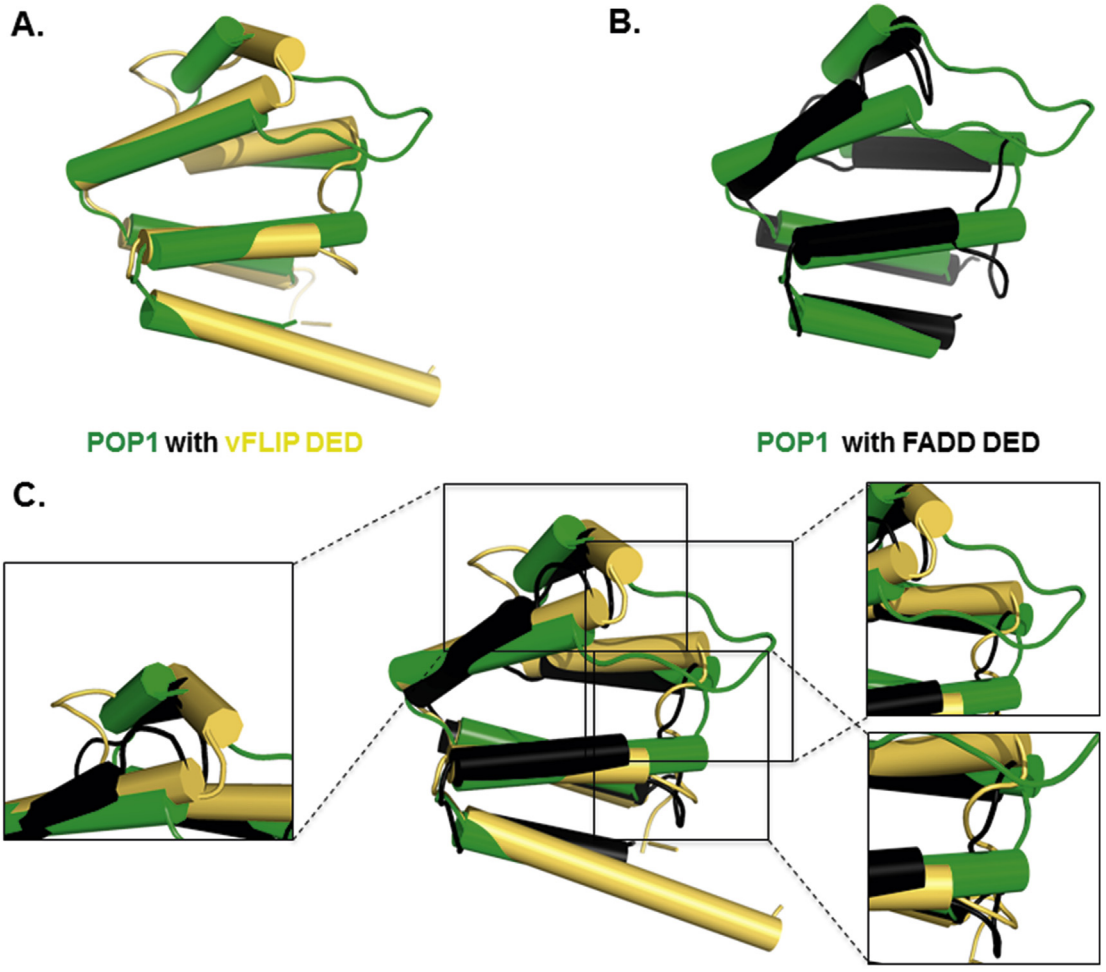

Fig. 3. Structural comparison with DEDs. Pairwise structural comparisons with DEDs were performed. A. POP1 (green) was superposed with vFLIP DED (yellow). B. POP1 (green) was superposed with FADD DED (black). C. Superposition of vFLIP DED and FADD DED. (For interpretation of the references to colour in this figure legend, the reader is referred to the web version of this article.)

long loop, residues 30–39 (H2–H3 loop), and four linkers connect the six helices. The two POP1 structures in the asymmetric unit form an asymmetric dimer. Few interaction forces were detected at the interaction interfaces. The total dimer surface buries 721 Å^2 (a monomer surface area of 360 Å^2), which represents 6.9% of the dimer surface area as calculated by PDBePISA [27].

Previously, the NMR structure of ASC2 was solved [28]. To determine the rigidity of the POP1 structure, we compared the current crystal structure with NMR structure by superposition. Superposition of the structures revealed that the orientation of H3 and H6 were slightly different, and the H2–H3 loop is not perfectly superposed, indicating that the POP1 structure is dynamic and that the structure can shift slightly in different conditions. This dynamic movement at H6, H3 and the connecting H2–H3 loop might be a common property of PYD and even DD superfamily. To better understand DD superfamily-mediated protein interactions, further structural studies are needed.

3.2. Comparison with other PYD structures

A structural homology search using the DALI server [29] revealed that the POP1 structure is highly similar to other PYD structures, although the sequence identity is low (less than 20–30% identity except for the ASC PYD) (Fig. 2A). The top eight selected matches, which had high Z-scores, were as follows: ASC PYD, NLRP3 PYD, NLRP4 PYD, NLRP7 PYD, NLRP12 PYD, vFLIP DED, NALP1 PYD, and FADD DED (Table 2). Interestingly, vFLIP DED and FADD DED were selected as the most structurally similar proteins outside of members of the PYD family.

Pairwise structural alignments between POP1 and other representative PYDs revealed that the helices and loops in PYDs differ slightly in length and orientation (Fig. 2B–F). When compared with NLRP4 PYD (Fig. 3D) and NALP1 PYD (Fig. 2F), helix H6 of POP1 showed differences in orientation. Differences in length were also detected compared to H2 of NLRP4 PYD. The greatest differences were detected at the loop connecting H2 and H3 (H2–H3 loop) (Fig. 2A). Specifically, the length and the orientation of the H3–H4 loop of PYDs varied, indicating that the loop is dynamic in solution. Unlike other PYDs, an additional helix in between H2 and H3 was detected in the NLRP7 PYD. In a previous study, the structure of NALP1 PYD lacked H3, which is observed in other PYD structures, indicating that the lack of H3 is unusual and might be an artifact (Fig. 2F).

3.3. Comparison with DED structure

The DD superfamily includes DDs, CARDs, DEDs, and PYDs. Classification of subfamily is based on their functional and structural similarities [12,30,31]. Six-helix bundle fold is the typical sturuture of DD superfamily [31]. Although they share structural similarity, several structural studies showed that each subfamily has unique structural characteristics, such as a more flexible and exposed third helix in the DDs, the presence of an RxDL motif in the DEDs, an interrupted first helix in the CARDs, and a relatively small third helix in the PYDs [32–34]. In current study, unexpectedly, two DED

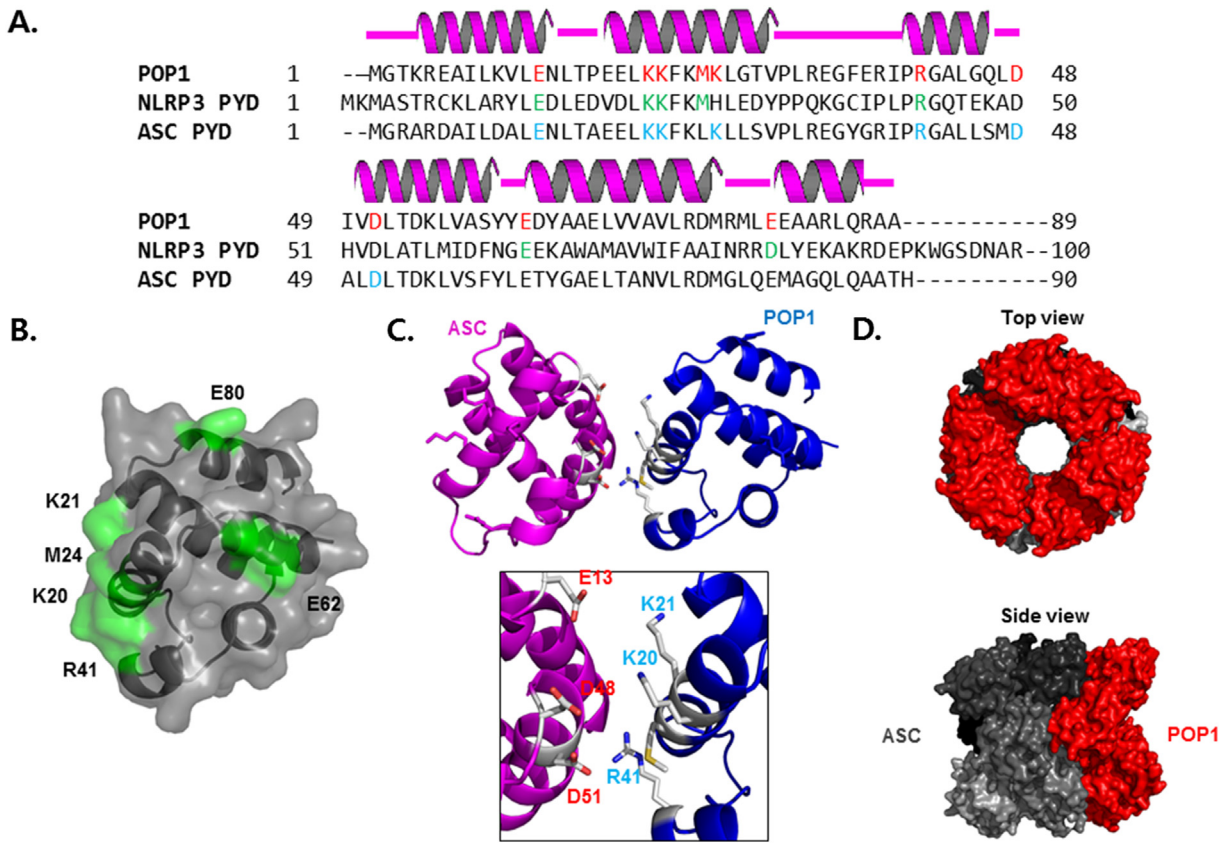

Fig. 4. A model of the proposed inhibitory mechanism of inflammasome formation by POP1. A. Alignment of PYD domain sequences from inflammasome components (NLRP3 and ASC) and POP1. The secondary structure elements are indicated above the sequence. Amino acids previously found to be important for the formation of the ASC PYD:NLRP3 PYD complex are colored in red for NLRP3 PYD and cyan for ASC PYD. Critical residues for the formation of the inflammasome that are conserved in POP1 are colored red. B. Conserved exposed residues that might be involved in the interaction with ASC and be critical to the function of POP1 are mapped on the structure of POP1. C. Model of 1:1 interaction between ASC and POP1. The interaction interface is magnified. D. Model of the multiple interaction mode that has been detected in the filament-like structure of NLRP3:ASC complex. (For interpretation of the references to colour in this figure legend, the reader is referred to the web version of this article.)

structures, vFLIP DED and FADD DED, were identified as structurally similar proteins to POP1 by the DALI server. Pairwise structural alignments between POP1 and vFLIP DED (Fig. 3A) and FADD DED (Fig. 3B) revealed that the structure of POP1 contains both structural similarities and differences. The differences are 1) POP1 and other PYDs contain a relatively long H2–H3 loop, 2) DEDs contain a relatively longer H4–H5 loop, and 3) the orientation of H3 varies throughout the subfamilies (Fig. 3C). Our study showed that the longer H2–H3 loop and shorter H4–H5 loop might be a distinct feature of PYDs.

3.4. A model of the inhibition mechanism of POP1

Because POP1 is known to be involved in the inhibition of inflammasome formation by tight interaction with ASC via a PYD–PYD interaction, we speculated on the molecular basis of this process using the reported filament-like structure of the ASC complex, which is a core part of the inflammasome [19]. The study showed that ASC forms a filament-like platform to recruit caspase-1 and NLRP3 that is critical for nucleating the assembly of ASC. NLRP3 amino acid residues M27, E64, D82, E15, K23, K24 and R43 on and ASC E13, K21, K22, K26, R41, D48, and D51 are critical to the assembly of the inflammasome. Based on sequence alignment, all the residues in NLRP3 that disrupt complex formation upon mutation are conserved in the POP1 sequence, indicating that the binding mode of POP1 and ASC is similar to that of NALP3 and ASC (Fig. 4A). Therefore, we mapped the mutations that disrupt the formation of the inflammasome on the POP1 structure (Fig. 4B). Based on this mapping study and a previous biochemical study, there are two possible inhibitory mechanisms of POP1. First because the basic patch on POP1 formed by K20, K21, and R41 is known to be critical for the interaction with ASC, POP1 could directly bind to ASC at a 1:1 ratio using this basic patch (Fig. 4C) [19,35]. Another possibility is that POP1 can nucleate the formation of the ASC filament, similar to NLRP3. The oligomeric POP1 binds to the top of the ASC filament and inhibits the recruitment of NLRP3 to ASC (Fig. 4D). In this case, POP1 would use multiple binding sites that have been identified in the filament-like structure of ASC and NALP3 [19].

Conflict of interest

The authors declare no conflict of interest.

Acknowledgments

This study was supported a grant from the Korea Healthcare Technology R&D project, Ministry of Health and Welfare, Republic of Korea (HI13C1449).

Transparency document

Transparency document related to this article can be found online at http://dx.doi.org/10.1016/j.bbrc.2015.03.134.

References

[1] T. Ghayur, S. Banerjee, M. Hugunin, D. Butler, L. Herzog, A. Carter, L. Quintal, L. Sekut, R. Talanian, M. Paskind, W. Wong, R. Kamen, D. Tracey, H. Allen, Caspase-1 processes IFN-gamma-inducing factor and regulates LPS-induced IFN-gamma production, Nature 386 (1997) 619–623.
[2] T.D. Kanneganti, N. Ozoren, M. Body-Malapel, A. Amer, J.H. Park, L. Franchi, J. Whitfield, W. Barchet, M. Colonna, P. Vandenabeele, J. Bertin, A. Coyle, E.P. Grant, S. Akira, G. Nunez, Bacterial RNA and small antiviral compounds activate caspase-1 through cryopyrin/Nalp3, Nature 440 (2006) 233–236.
[3] F.S. Sutterwala, Y. Ogura, M. Szczepanik, M. Lara-Tejero, G.S. Lichtenberger, E.P. Grant, J. Bertin, A.J. Coyle, J.E. Galan, P.W. Askenase, R.A. Flavell, Critical role for NALP3/CIAS1/Cryopyrin in innate and adaptive immunity through its regulation of caspase-1, Immunity 24 (2006) 317–327.
[4] L. Franchi, T. Eigenbrod, R. Munoz-Planillo, G. Nunez, The inflammasome: a caspase-1-activation platform that regulates immune responses and disease pathogenesis, Nat. Immunol. 10 (2009) 241–247.
[5] K. Schroder, J. Tschopp, The inflammasomes, Cell 140 (2010) 821–832.
[6] J.Y. Bae, H.H. Park, Crystal structure of NALP3 protein pyrin domain (PYD) and its implications in inflammasome assembly, J. Biol. Chem. 286 (2011) 39528–39536.
[7] F. Martinon, Detection of immune danger signals by NALP3, J. Leukoc. Biol. 83 (2008) 507–511.
[8] J.A. Duncan, D.T. Bergstralh, Y. Wang, S.B. Willingham, Z. Ye, A.G. Zimmermann, J.P. Ting, Cryopyrin/NALP3 binds ATP/dATP, is an ATPase, and requires ATP binding to mediate inflammatory signaling, Proc. Natl. Acad. Sci. U. S. A. 104 (2007) 8041–8046.
[9] H.H. Park, Y.C. Lo, S.C. Lin, L. Wang, J.K. Yang, H. Wu, The death domain superfamily in Intracellular signaling of apoptosis and inflammation, Ann. Rev. Immunol. 25 (2007) 561–586.
[10] H.H. Park, PYRIN domains and their interactions in the apoptosis and inflammation signaling pathway, Apoptosis 17 (2012) 1247–1257.
[11] H.H. Park, Structural analyses of death domains and their interactions, Apoptosis 16 (2011) 209–220.
[12] D. Kwon, J.H. Yoon, S.Y. Shin, T.H. Jang, H.G. Kim, I. So, J.H. Jeon, H.H. Park, A comprehensive manually curated protein-protein interaction database for the death domain superfamily, Nucleic Acids Res. 40 (2012) D331–D336.
[13] B.K. Davis, H. Wen, J.P. Ting, The inflammasome NLRs in immunity, inflammation, and associated diseases, Annu. Rev. Immunol. 29 (2011) 707–735.
[14] L. Agostini, F. Martinon, K. Burns, M.F. McDermott, P.N. Hawkins, J. Tschopp, NALP3 forms an IL-1beta-processing inflammasome with increased activity in Muckle-Wells autoinflammatory disorder, Immunity 20 (2004) 319–325.
[15] A. Dorfleutner, N.B. Bryan, S.J. Talbott, K.N. Funya, S.L. Rellick, J.C. Reed, X. Shi, Y. Rojanasakul, D.C. Flynn, C. Stehlik, Cellular pyrin domain-only protein 2 is a candidate regulator of inflammasome activation, Infect. Immun. 75 (2007) 1484–1492.
[16] C. Stehlik, A. Dorfleutner, COPs and POPs: modulators of inflammasome activity, J. Immunol. 179 (2007) 7993–7998.
[17] A. Dorfleutner, S.J. Talbott, N.B. Bryan, K.N. Funya, S.L. Rellick, J.C. Reed, X. Shi, Y. Rojanasakul, D.C. Flynn, C. Stehlik, A shope fibroma virus PYRIN-only protein modulates the host immune response, Virus Genes. 35 (2007) 685–694.
[18] J.B. Johnston, J.W. Barrett, S.H. Nazarian, M. Goodwin, D. Ricciuto, G. Wang, G. McFadden, A poxvirus-encoded pyrin domain protein interacts with ASC-1 to inhibit host inflammatory and apoptotic responses to infection, Immunity 23 (2005) 587–598.
[19] A. Lu, V.G. Magupalli, J. Ruan, Q. Yin, M.K. Atianand, M.R. Vos, G.F. Schroder, K.A. Fitzgerald, H. Wu, E.H. Egelman, Unified polymerization mechanism for the assembly of ASC-dependent inflammasomes, Cell 156 (2014) 1193–1206.
[20] K.H. Do, H.H. Park, Crystallization and preliminary X-ray crystallographic studies of cPOP1, Acta Crystallogr. Sect. F. Struct. Biol. Cryst. Commun. 69 (2013) 292–294.
[21] W.A. Hendrickson, J.R. Horton, D.M. LeMaster, Selenomethionyl proteins produced for analysis by multiwavelength anamalous diffraction (MAD): a vehicle for direct determination of three dimensional structure, EMBO J. 9 (1990) 1665–1672.
[22] Z. Otwinowski, DENZO Data Processing Package, Yale University, C.T, 1990.
[23] G.M. Sheldrick, A short history of SHELX, Acta Crystallogr. A 64 (2008) 112–122.
[24] T. Terwilliger, SOLVE and RESOLVE: automated structure solution, density modification and model building, J. Synchrotron Radiat. 11 (2004) 49–52.
[25] P. Emsley, K. Cowtan, Coot: model-building tools for molecular graphics, Acta Crystallogr. D. Biol. Crystallogr. 60 (2004) 2126–2132.
[26] P.V. Afonine, R.W. Grosse-Kunstleve, P.D. Adams, A robust bulk-solvent correction and anisotropic scaling procedure, Acta Crystallogr. D. Biol. Crystallogr. 61 (2005) 850–855.
[27] E. Krissinel, K. Henrick, Inference of macromolecular assemblies from crystalline state, J. Mol. Biol. 372 (2007) 774–797.
[28] A. Natarajan, R. Ghose, J.M. Hill, Structure and dynamics of ASC2, a pyrin domain-only protein that regulates inflammatory signaling, J. Biol. Chem. 281 (2006) 31863–31875.
[29] L. Holm, C. Sander, Dali: a network tool for protein structure comparison, Trends Biochem. Sci. 20 (1995) 478–480.
[30] J.C. Reed, K.S. Doctor, A. Godzik, The domains of apoptosis: a genomics perspective, Sci. STKE 2004 (2004) re9.
[31] K. Kersse, J. Verspurten, T. Vanden Berghe, P. Vandenabeele, The death-fold superfamily of homotypic interaction motifs, Trends Biochem. Sci. 36 541–552.
[32] K. Hofmann, P. Bucher, J. Tschopp, The CARD domain: a new apoptotic signalling motif, Trends Biochem. Sci. 22 (1997) 155–156.
[33] F. Martinon, K. Hofmann, J. Tschopp, The pyrin domain: a possible member of the death domain-fold family implicated in apoptosis and inflammation, Curr. Biol. 11 (2001) R118–R120.
[34] H.H. Park, E. Logette, S. Rauser, S. Cuenin, T. Walz, J. Tschopp, H. Wu, Death domain assembly mechanism revealed by crystal structure of the oligomeric PIDDosome core complex, Cell 128 (2007) 533–546.

[35] T. Srimathi, S.L. Robbins, R.L. Dubas, H. Chang, H. Cheng, H. Roder, Y.C. Park, Mapping of POP1-binding site on pyrin domain of ASC, J. Biol. Chem. 283 (2008) 15390–15398.
[36] E. Liepinsh, R. Barbals, E. Dahl, A. Sharipo, E. Staub, G. Otting, The death-domain fold of the ASC PYRIN domain, presenting a basis for PYRIN/PYRIN recognition, J. Mol. Biol. 332 (2003) 1155–1163.
[37] C. Eibl, S. Grigoriu, M. Hessenberger, J. Wenger, S. Puehringer, A.S. Pinheiro, R.N. Wagner, M. Proell, J.C. Reed, R. Page, K. Diederichs, W. Peti, Structural and functional analysis of the NLRP4 pyrin domain, Biochemistry 51 (2012) 7330–7341.
[38] A.S. Pinheiro, M. Proell, C. Eibl, R. Page, R. Schwarzenbacher, W. Peti, Three-dimensional structure of the NLRP7 pyrin domain: insight into pyrin-pyrin-mediated effector domain signaling in innate immunity, J. Biol. Chem. 285 (2010) 27402–27410.
[39] A.S. Pinheiro, C. Eibl, Z. Ekman-Vural, R. Schwarzenbacher, W. Peti, The NLRP12 pyrin domain: structure, dynamics, and functional insights, J. Mol. Biol. 413 (2011) 790–803.
[40] J.K. Yang, L. Wang, L. Zheng, F. Wan, M. Ahmed, M.J. Lenardo, H. Wu, Crystal structure of MC159 reveals molecular mechanism of DISC assembly and FLIP inhibition, Mol. Cell. 20 (2005) 939–949.
[41] S. Hiller, A. Kohl, F. Fiorito, T. Herrmann, G. Wider, J. Tschopp, M.G. Grutter, K. Wuthrich, NMR structure of the apoptosis- and inflammation-related NALP1 pyrin domain, Structure 11 (2003) 1199–1205.
[42] M. Eberstadt, B. Huang, Z. Chen, R.P. Meadows, S.-C. Ng, L. Zheng, M.J. L, S.W. Fesik, NMR structure and mutagenesis of the FADD (Mort1) death-effector domain, Nature 392 (1998) 941–945.